Cement and Concrete Research 42 (2012) 558–566

Contents lists available at SciVerse ScienceDirect

Cement and Concrete Research

journal homepage: http://ees.elsevier.com/CEMCON/default.asp

Hardened properties of high-performance printing concrete

T.T. Le *, S.A. Austin, S. Lim, R.A. Buswell, R. Law, A.G.F. Gibb, T. Thorpe

Department of Civil and Building Engineering, Loughborough University, Loughborough, Leicestershire, LE11 3TU, United Kingdom

ARTICLE INFO

Article history:
Received 19 July 2011
Accepted 12 December 2011

Keywords:
Additive manufacturing
Bond strength (C)
Compressive strength (C)
High-performance concrete (E)
Tensile properties (C)

ABSTRACT

This paper presents the hardened properties of a high-performance fibre-reinforced fine-aggregate concrete extruded through a 9 mm diameter nozzle to build layer-by-layer structural components in a printing process. The printing process is a digitally controlled additive method capable of manufacturing architectural and structural components without formwork, unlike conventional concrete construction methods. The effects of the layering process on density, compressive strength, flexural strength, tensile bond strength and drying shrinkage are presented together with the implication for mix proportions. A control concrete (mould-cast specimens) had a density of approximately 2250 kg/m^3, high strength (107 MPa in compression, 11 MPa in flexure) and 3 MPa in direct tension, together with a relatively low drying shrinkage of 175 μm (cured in water) and 855 μm (cured in a chamber at 20 °C and 60% relative humidity) at 184 days. In contrast well printed concrete had a density of 2350 kg/m^3, compressive strength of 75–102 MPa, flexural strength of 6–17 MPa depending on testing direction, and tensile bond strength between layers varying from 2.3 to 0.7 MPa, reducing as the printing time gap between layers increased. The well printed concrete had significantly fewer voids greater than 0.2 mm diameter (1.0%) when compared with the mould-cast control (3.8%), whilst samples of poorly printed material had more voids (4.8%) mainly formed in the interstices between filaments. The additive extrusion process was thus shown to retain the intrinsic high performance of the material.

1. Introduction

A high performance printing concrete has been developed for an innovative freeform-construction concrete-printing process [1,2]. The concrete used some advantages of self-compacting concrete [3,4] and sprayed concrete [5,6] for optimisation of the mix proportions to suit the innovative process. The concrete printing process and the fresh properties of the concrete, including the optimisation of mix proportions, extrudability, workability, open time and buildability are reported elsewhere [7,8].

The concrete printing process uses an additive, layer-based, manufacturing technique to build complex geometrical shapes without formwork and thus has a unique advantage over conventional construction methods. Additive manufacturing (AM) has been applied to the production of cement composites such as Contour Crafting [9] and D-Shape (Monolite) [10]. Contour Crafting is based upon extruding a cement-based paste against a trowel that creates a smooth surface finish through the buildup of subsequent layers. The D-Shape involves a powder deposition process, where each layer of building material is deposited to the desired thickness, compacted and then nozzles mounted on a gantry frame deposit the binder where the part is to be made solid. Other applications of AM include the medical field [11–13]. For instance, AM techniques using cement-based materials such as fibre reinforced bone cement have been used for bone tissue implantation aiming to replace and/or repair bone defects due to traumatised, damaged or lost bone [12]. These might also be used for making heart valves [12]. Other research is developing several cement-based materials to overcome the poor water resistance of commercially available materials, which is problematic for applications including biomedical processing [13].

Briefly, in the concrete printing process, components are designed as volumetric objects using 3D modelling software. They are sliced and represented as a series of two dimensional layers. The data are exported to a printing machine layer-by- to print structural components by the controlled extrusion of a concrete. The rheology must allow its extrusion through a printing head incorporating a 9 mm diameter nozzle to form small concrete filaments. As they are laid, the filaments bond together to form each layer and to the previous layers to build 3D components.

The layered structure is likely to be anisotropic as voids can form between filaments to weaken the structural capability. The bond between filaments, as well as between layers, probably influences the hardened properties of concrete components. Therefore, a high strength in compression and flexure as well as tensile bond is the main target in developing this concrete. Additionally, a low shrinkage is essential as the freeform components are built without formwork and this could accelerate water evaporation in the concrete and result in cracking.

* Corresponding author. Current address: National University of Civil Engineering in Hanoi, Vietnam (NUCE). Tel.: +84 942015290; fax: +84 438691684.
E-mail address: lttnvn@gmail.com (T.T. Le).

0008-8846/$ – see front matter © 2011 Elsevier Ltd. All rights reserved.
doi:10.1016/j.cemconres.2011.12.003

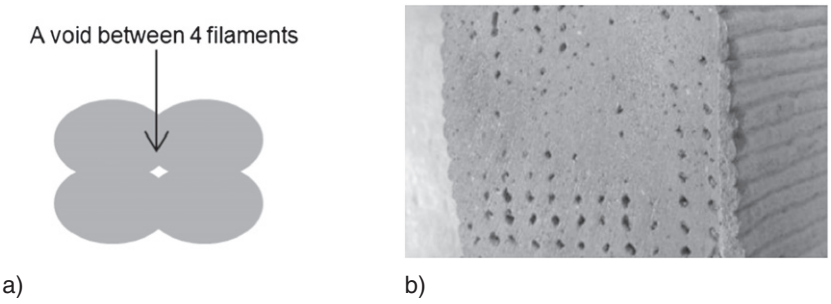

Fig. 1. Voids formed between filaments resulting from a poorly executed printing process. a) Four filaments may form a void. b) Poor printing example with obvious voids between filaments.

This paper presents the hardened properties comprising density, compressive and flexural strengths, tensile bond strength and drying shrinkage. Void measurement was also carried out to further understand the hardened properties. It compares the performance of conventionally cast (the control) and in-situ printed states, considering where appropriate the anisotropy resulting from the extrusion process.

2. Experimental programme

2.1. Specimen manufacture

In this research, the specimens were manufactured in both mould-cast and printed states. The test results would show clearly the impact of the concrete printing process on the hardened properties of concrete.

2.1.1. Mould cast control samples

All control specimens were cast in moulds and complied with the respective BS EN standards used to measure the properties. Compressive strength specimens were cast in 100 mm cube steel moulds complied with BS EN 12390–3:2009 [14]. Flexural strength specimens were cast in 100×100×500 mm steel moulds complied with BS EN 12390–5:2009 [15]. Tensile strength specimens were cored from 150 mm mould-cast cubes to comply with BS EN 14488–4:2005 + A1:2008 [16]. Shrinkage specimens were cast in 75×75×220 mm steel moulds in accordance with BS EN 12617–4:2002 [17].

2.1.2. Printed samples

The printed specimens were manufactured by sawing and coring from printed components including 350×350×120 mm slabs, 500x350x120mm slabs, a trial curvy-shape bench with 2000/1000/63 mm length/width/thickness and 500×100×200 mm beams (see Experimental procedures section).

Table 1
The chemical composition of cement CEM I 52.5, fly ash and silica fume.

Component	Average percentage by weight (%)		
	Cement CEM I 52.5	Fly ash	Silica fume
SiO_2	19.4–21.5	45–51	90–97
Al_2O_3	4.1–4.9	27–32	
Fe_2O_3	2.7–2.9	7–11	
CaO	61.9–64.0	1–5	
MgO	1.1–1.2	1–4	
SO_3	3.0–3.2	0.3–1.3	
K_2O	0.6–0.7	1–5	
Na_2O	0.2	0.8–1.7	
TiO_2		0.8–1.1	
Cl	0.04–0.05	0.05–0.15	
Loss of ignition	2.3–4.1		<3.0

As expected, the process had the potential to create small voids in the interstices between the filaments (Fig. 1(a)). A cross section of a poorly manufactured specimen is shown in Fig. 1(b). Careful design and control of the mix rheology and printing process avoids such macro effects, but the sample serves to illustrate the potential for longitudinal flaws and the resulting anisotropy that this paper explores.

2.2. Materials and mix proportions

The mix design aimed to meet the requirements of both the fresh and hardened states. The former comprises printability, workability, open time and buildability. The hardened performance includes the compressive and flexural strengths of both cast and printed specimens. The mix design targeted a compressive strength of over 100 MPa and a flexural strength of over 10 MPa at 28 days for mould-cast specimens. A 2 mm maximum size sand was selected because of the small nozzle diameter (9 mm) required to give a high printing resolution; cement CEM I 52.5, fly ash conforming to BS EN 450 and undensified silica fume formed the binder component. The chemical composition of cement, fly ash and silica fume are shown in Table 1.

The gradings of sand, cement, fly ash and silica fume, measured by a Mastersizer 2000 machine, were combined in various proportions to form smooth grading curves of potential mixtures. Further details of the raw materials used and the potential mixtures designed are shown in Fig. 2.

Dry components were mixed with water and a polycarboxylate-based superplasticiser to lower the water/binder ratio and hence increase its workability and strength. A retarder, formed by amino-tris (methylenephosphonic acid), citric acid and formaldehyde, maintained sufficient open time, facilitating a constant flow during printing. The concrete also contained 12/0.18 mm length/diameter polypropylene micro fibres to reduce the possibility of plastic

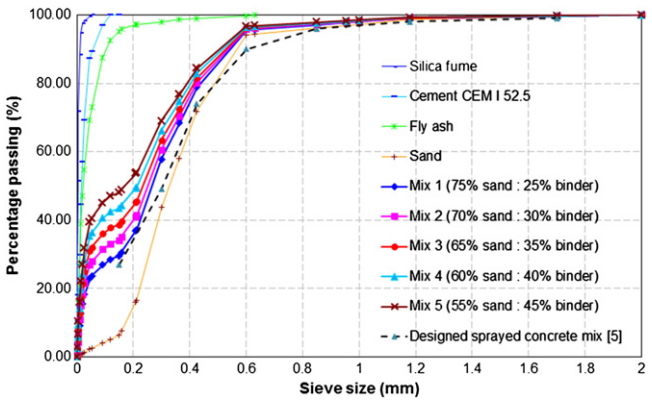

Fig. 2. Particle size distribution of raw materials and potential mixtures.

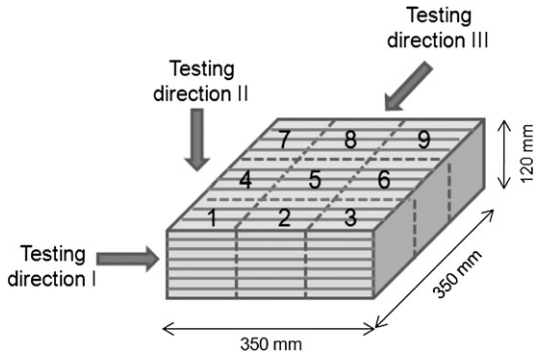

Fig. 3. Cutting diagram and testing directions for nine 100 mm cube specimens extracted from the 350×350×120 mm slab.

shrinkage. The optimum mix was found to be one with the lowest content of binder that could be printed and built with the recommended dosage of fibres from the supplier (i.e. 1.2 kg/m^3) that gained the target strengths.

The optimisation process resulted in a mix with a 60:40 sand: binder ratio, comprising 70% cement, 20% fly ash and 10% silica fume, plus 1.2 kg/m^3 micro polypropylene fibres [7,8]. The water: binder ratio was 0.26 and the water–cement ratio was therefore 0.37. This mix required 1% superplasticiser and 0.5% retarder to attain an optimum workability of 0.55 kPa shear strength, an optimum open time of up to 100 min and the ability to build a large number of layers with various filament groups. The compressive strength of this mix, determined by casting 100 mm cube specimens, was 20, 80, 107 and 125 MPa, at 1, 7, 28 and 56 days respectively. A variety of parts were printed with mould-cast controls, and specimens extracted to determine the effects of this AM process on key properties, namely density, compressive strength, flexural strength, tensile bond strength and drying shrinkage. Except where stated, all properties reported are with these mix proportions.

2.3. Experimental procedures

2.3.1. Density

The density of mould-cast and printed specimens were averaged from at least three specimens, the former complying with BS EN 12390–7:2009 [18]. For printed concrete, 100 mm cube specimens were sawn from 350×350×120 mm and 500×350×120 mm printed slabs to measure the density as for the mould-cast specimens. The results were verified with 58 mm diameter cores in the investigation of tensile bond strength.

2.3.2. Compressive strength

Compressive strength was measured in both mould-cast and printed specimens. Most specimens were 100 mm cubes. Mould-cast specimens were cured in a 20 °C water tank and tested at 1, 7 and 28 day ages to monitor the strength development with time.

For printed elements, 100 mm cube specimens were extracted from one 350×350×120 mm slab and three 500×350×120 mm slabs (Figs. 3 and 5). The slabs were cured under damp hessian, wrapped in plastic sheeting. Nine cubes were extracted from the 350×350×120 mm slab and loaded in one of three directions: direction I for specimens 1–3; direction II for specimens 4–6; and direction III for specimens 7–9 (Fig. 3). Nine cubes extracted from three 500×350×120 mm slabs were tested at the same loading directions of the flexural beam specimens (Fig. 5).

All 100 mm cube specimens were tested in accordance with BS EN 12390–3:2009 [14]. Printed specimens were capped with a high strength gypsum-based plaster.

Additionally, fifteen 58 mm diameter cores, fifteen 63 mm cut cubes and ten 50×220 mm width x length prisms were extracted from a 63 mm thick trial print of a curved component to understand the performance of printed concrete under compressive and flexural loading (Fig. 4). All cylinder were tested perpendicular to the printing surface whilst cube specimens were tested in three orientations: 3 perpendicular with a cut surface (loading direction I), 9 perpendicular to the printing surface (loading direction II) and 3 perpendicular with a side surface (loading direction III), as shown top-right of Fig. 4. The loading rate was also 0.4 N/mm^2. The full-scale print of the bench has been shown in elsewhere [7,8].

2.3.3. Flexural strength

Flexural strength was also measured in both mould-cast and printed states. 100×100×500 mm slabs were mould-cast, removed after one day and then cured in a 20 °C water tank up to 28 days. For printed specimens, three 500×350×120 mm slabs were printed and cured under damp hessian. Three 100×100×400 mm beams and three 100 mm cubes were extracted from each slab at 28 day age. Slabs 1 and 2 were printed and cut as depicted in Fig. 5a whilst slab 3 was printed and cut as depicted in Fig. 5b. Cube and beam specimens extracted from slabs 1, 2 and 3 were tested in directions I, II and III, respectively.

All beam specimens were tested under 4-point bending with a span of 300 mm, complying with BS EN 12390–5:2009 [15]. An additional ten 50×63×220 mm beam specimens extracted from the trial printed component (Fig. 4) were also tested to further understand anisotropy of the flexural performance of printed concrete.

2.3.4. Tensile bond strength

A critical characteristic of this printing process is the bond between layers, which can influence the structural performance, particularly when the process temporarily stops between layers. The influence of time between printing layers was investigated (in increments of 15, 30 min, 1, 2, 4, 8, 18 h and 1, 3, 7 days) by a direct tension test on cylindrical cored specimens. The direct tensile strength

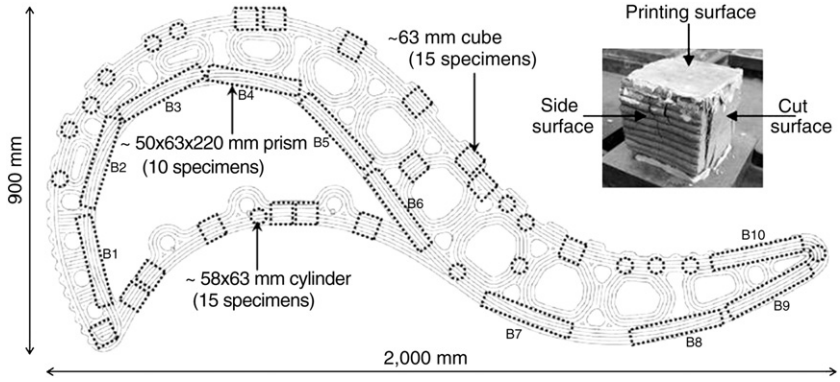

Fig. 4. Diagram showing positions of extracting printed specimens from a multi-cellular curved bench and typical cube specimen.

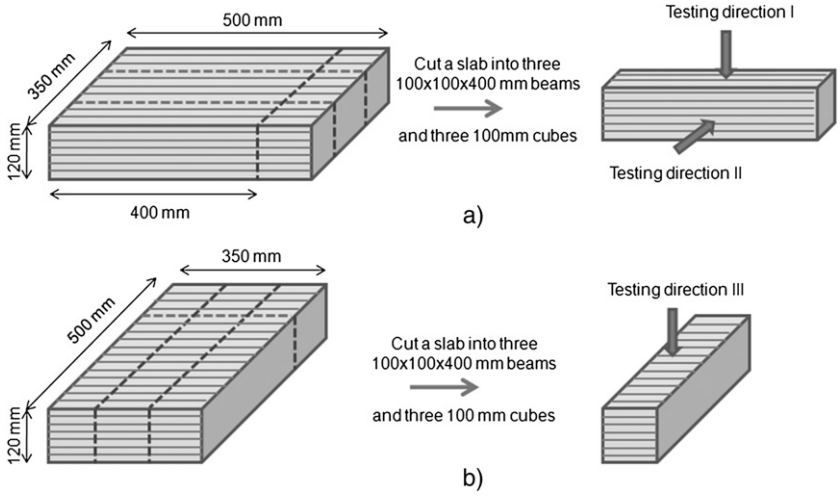

Fig. 5. Diagram of cutting slabs and testing flexural strength.

was also measured as a control using the same size of specimens and testing procedures.

To prepare the cored cylinder specimens, a 100×100×500 mm beam was printed. Then, after a time gap, another 100×100×500 mm beam was printed on top. The components were then covered with damp hessian and plastic sheeting for a day before being moved to a laboratory storage area where the same curing regime was maintained up to 28 days. Six 58 mm diameter×120 mm height cylinder specimens were cored at the middle of each bonded beam component (Fig. 6).

The cored cylinder specimens were tested in accordance with BS EN 14488–4:2005 + A1:2008 [16]. Two 58×25 mm diameter×thickness steel dollies were glued to the ends of each cylinder specimen with a rapid curing, high strength adhesive.

2.3.5. Void measurement

One of the characteristics of this concrete printing process is the voids that can form between filaments (Fig. 1), which might affect the hardened properties significantly. The voids in the range of 0.2–4.0 mm size were quantified using "Image Tool" processing and analysis software to better understand the effects on the hardened performance of the printing concrete.

Void measurement was carried out in three specimen groups of mould-cast, poor printing and good printing (Fig. 7), each specimen having a 90×90 mm^2 surface.

Surfaces were cleaned and sprayed with a black paint. Once dry, a white paint was rolled on to reveal the voids that retained the black colour. The surface was subsequently scanned and the image transferred to a void measuring software "Image Tool" which counted the number of voids and their area.

2.3.6. Drying shrinkage

As the printing process fabricates without formwork, the surface area in contact with air is large and this could accelerate drying shrinkage due to water evaporation, and consequently increase the risk of cracking. Mould cast 75×75×229 mm beams complying with BS EN 12617–4:2002 [17] were monitored over six months in three curing conditions: water immersed, covered in damp hessian with a plastic sheet wrapped and in a climatic chamber (20 °C and 60% relative humidity). Each group comprised five specimens.

3. Results and discussion

3.1. Density

The average density (mould-cast) of the optimum mix was 2250 kg/m^3 Whilst that of well-printed specimens was a little higher at 2350 kg/m^3 This was probably because the concrete hopper was gently vibrated before delivery of the fresh concrete, and the pipe and pump system also provided a small pressure during extrusion. A similar trend occurred in a previous study on wet-spayed mortars [19,20]. Although this high performance printing concrete has only a sand aggregate, the density is much higher than that of ordinary mortars (1800 kg/m^3) and sprayed mortars [19] (i.e. 1800–2000 kg/m^3 on average). The high density is also attributed to the grading and homogeneity resulting in high strengths and low shrinkage.

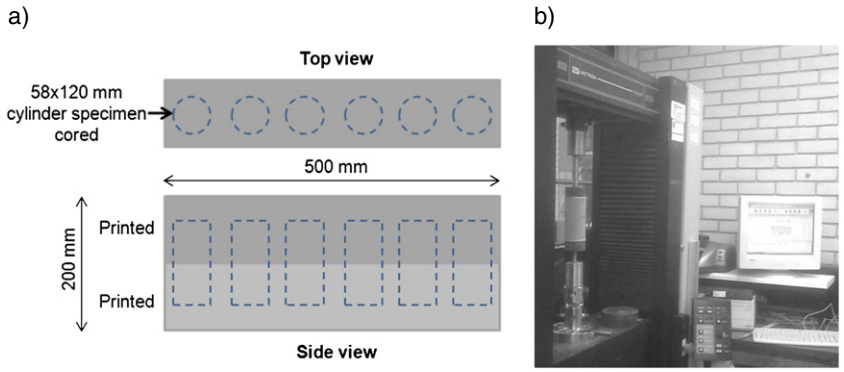

Fig. 6. Arrangement for testing tensile bond strength. a) Coring six 58×120 mm cylinder specimens from a beam bond component. b) Testing tensile bond strength.

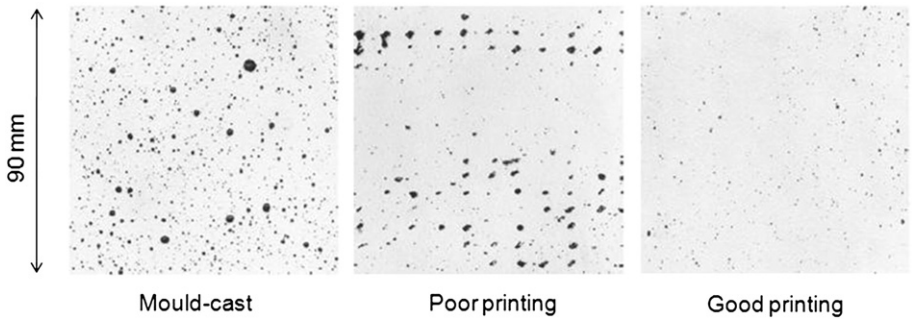

Fig. 7. Three typical specimens for void measurement.

3.2. Compressive strength

The mould-cast cube compressive strength at 28 days was typically 107 MPa but varied with the admixtures and their dosages. The superplasticiser appeared to delay the hardening of concrete at an early age. However, as expected and also in agreement with previous work [21,22], at 7 days and 28 days the specimens with 1–2% superplasticiser had higher strength compared with 0.5% superplasticiser. Without superplasticiser the fresh concrete became stiff and then could not be printed so the compressive strength was not determined. Over 1% retarder reduced significantly the compressive strength at early ages, i.e. 1 and 7 days. Indeed 1.5–2% retarder resulted in no measurable compressive strength at 1 day. By 28 days, the retarder effect appeared to have disappeared, the compressive strengths of all mixes being approximately 100 MPa. The accelerator increased the compressive strength at one day significantly: by 70% with 3–5% and 40% with 1% accelerator. However, by 7 days, this enhancement had disappeared and by 28 days the strengths of 3–5% accelerator specimens were lower than that of 1% accelerator specimens.

Testing of printed samples in various directions relative to the layers revealed a strength from 75 to 102 MPa (see Fig. 8 which includes a comparison with mould cast equivalents).

Key:

SD standard 100 mm mould-cast cubes
S3I, S3II, S3III 100 mm cubes extracted from the 350x350x120 mm slab, tested in loading direction I, II and III (see Fig. 3)
S5I, S5II, S5III 100 mm cubes extracted from three 500x350x120 mm slabs, tested in loading direction I, II and III (see Fig. 5)
Bcy 58×63 mm cylinders cored from the trial curvy bench, (see Fig. 3)
BcuI, BcuII, BcuIII 63 mm cubes extracted from the trial curvy bench, tested in loading direction I, II and III (see Fig. 4)

The average compressive strengths of the 100 mm cube specimens extracted from a 350×350×120 mm slab were 102 MPa in direction I (specimens 1, 2, 3) and the same in direction II (specimens 4, 5, 6). In direction III it was 91 MPa (specimens 7, 8, 9). Compared with the standard mould-cast compressive strength, the printed concrete strength was similar in directions I and II and 15% lower in direction III. The nine 100 mm cube specimens tested in the series of three 500×350×120 mm slabs, depicted in Fig. 5, had an average compressive strengths of 97 MPa in direction I and 93 MPa in directions II and III. The printed strength was thus 9% lower in direction I and 13% lower in directions II and III, respectively. The results confirmed that a correctly executed extrusion process introduces relatively little anisotropy in terms of compressive strength, although it appears that loading in the plane of the layers (directions II and III) can reveal a small reduction, presumably associated with shear induced by platen friction exploiting any flaws at the bead boundaries.

However, the compressive strength reduced in the samples extracted from the print of the curvy shape (the series of fifteen 58×120 mm cylinders and fifteen 63 mm cube specimens). The equivalent cube compressive (converted using BS EN 12504:1–2009 [23] and an empirical relation [24]) varied from 75 to 83 MPa, i.e. up 30% less than the control. Additionally, the coefficients of variation of printed specimens of 17–20% were significantly higher than that of standard cubes (2%). Observation from the testing of this series revealed voids between the curved filaments that are likely to have been the cause of the lower compressive capacity.

3.3. Flexural strength

The average flexural strength of the mould-cast beams was 11 MPa (Fig. 9), i.e. approximately 10%, of compressive strength, agreeing with other research on high strength concretes [25–27].

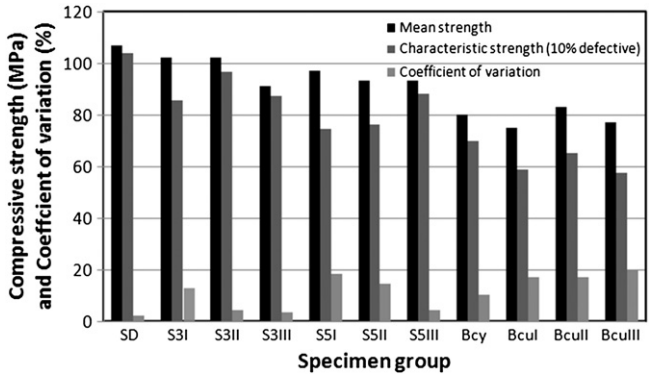

Fig. 8. Equivalent 100 mm cube compressive strengths of printed concretes compared with mould-cast specimens.

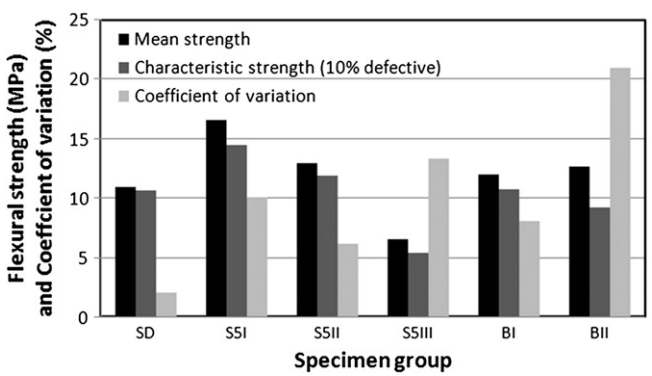

Fig. 9. Flexural strengths of printed concrete compared with standard mould-cast concrete.

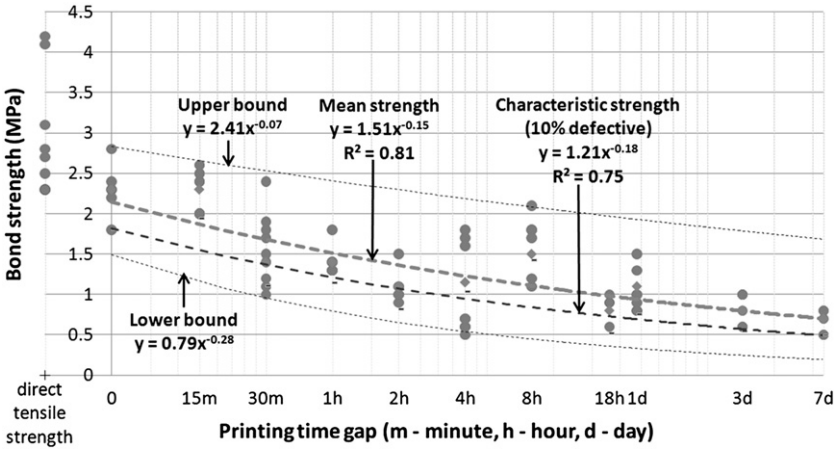

Fig. 10. Variation of tensile bond strength with printing gap and comparison with direct tensile strength.

Key:

SD standard 500x100x100 mm mould-cast beams

S5I, S5II, S5III 400x100x100 mm beams extracted from three 500x350x120 mm slabs, tested in loading direction I, II and III (Fig. 5)

BI, BII 220x63x50 mm beams extracted from the trial curvy bench, tested in loading direction I and II (Fig. 4)

The flexural strength of printed concrete varied with testing orientation. In the series extracted from three slabs 500×350×120 mm, the strengths in loading directions I and II (16 and 13 MPa respectively), were higher than that of the standard mould cast material (11 MPa). The flexural strength is determined by the central bottom area of beam specimens where the maximum tensile stress occurs. The concrete that carried load in the testing direction I was at the bottom of the slab printed and this area was probably well-compacted. The water-binder ratio of the lower concrete layers would also have been reduced if water bled out of the base layer. The combined effect would increase the loading capacity of the lower layers resulting in a higher flexural strength. The beams tested in direction III had a much lower average strength (7 MPa). This is because of the anisotropy resulting from the printing process where, in this case, the load was applied in the plane of the boundaries between filaments and the strength is thus highly dependent on the inter-layer bond strength.

The flexural strength of smaller printed beams extracted from the curvy component was slightly higher than the control. The mean strength of 5 beams loaded in direction I was 12 MPa and of 5 beams in direction II was 13 MPa. However these values are lower than in the same directions of the printed slabs reflecting the variation in printing quality and following the same trend as for compressive strength. This is reinforced by the coefficients of variation of the printed specimens of up to 21% which were much larger than that of the mould-cast standard (2%).

3.4. Tensile bond strength

The tensile bond strength was investigated with 11 groups of specimens with a varying time gap between the older and newer part. The results are compared with the direct tensile strength of similar specimens and testing procedure in Fig. 10.

The results were quite variable, with coefficients of variation of 5 to 30%. This was expected given the nature of the layered extrusion process and the well established more general discussions concerning measurement of direct tensile strength [25] and tensile bond testing of concrete repairs [28]. It is thought that such specimens are more seriously affected by non-uniform shrinkage in comparison with other types of test specimens.

The failure stress was lower than the average tensile strength of 3.0 MPa, reducing on average from 2.3 MPa with printing time gaps of 0 and 15 min to 0.7 MPa for the 7 day gap. The specimens with a 0 and 15 minute time gap failed in the material (Fig. 11a) and thus the bond strength could not be determined but is higher than the measured values.

All specimens with a gap over 15 min failed at the interface between older and newer parts (Fig. 11b). Between a 30 minute and 7 day time gap the average bond strength was 53% and 77% lower than the control. This reduction with increasing gap in printing time was expected as the adhesion reduced. However, most of the results comfortably exceeded the Concrete Society recommended minimum bond strength of 0.8 MPa [19], and are well above the 0.4 to 0.9 MPa in a case study of a high performance concrete bridge deck overlay [29]. They are similar to published bond strengths of repair mortars and concretes of 0.8 to 2.3 MPa [19,28,30]. The trend lines

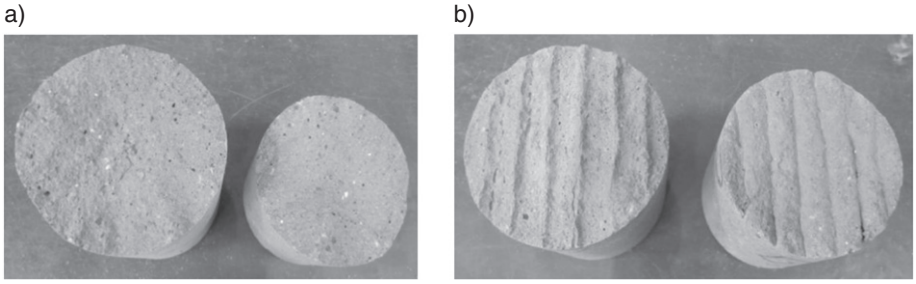

Fig. 11. Failure mode (broken surfaces) of tensile bond specimens. a) 15 minute gap specimen. b) 4 hour gap specimen.

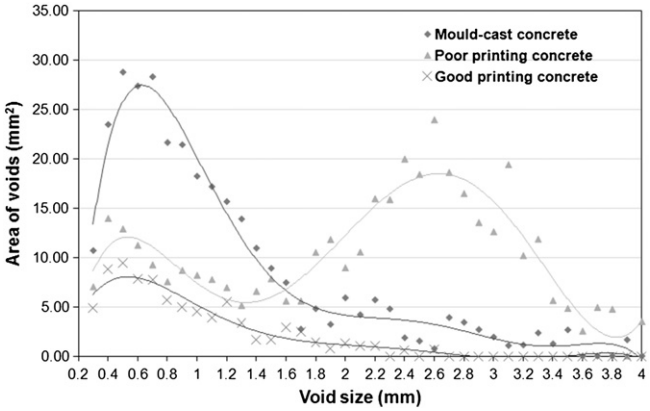

Fig. 12. Distribution of voids in three concrete groups.

suggest that characteristic bond strengths of 0.8, 1.0 and 1.2 MPa will be achieved with time gaps of 8, 3 and 1 h respectively. A more demanding 1.5 MPa would restrict the printing time per layer to around 15 min.

3.5. Void structure

The anisotropy affecting the hardened properties including the compressive, flexural and tensile bond behaviour was supported by the results of the void measurement. These revealed 3.8% voids (0.2–4.0 mm size) in mould-cast specimens whilst 4.8% formed in the poorly printed concrete and only 1.0% voids in the well printed concrete. Respectively, the density results were 2250, 2260 and 2350 kg/m^3 for mould-cast, poor printing and good printing. Although the void content of the poorly printed concrete (4.8%) was greater than that of the mould-cast (3.8%) the density was higher, implying a higher density. The content of voids less than 0.2 mm diameter in the printed concrete is likely to be smaller than that of mould-cast concrete.

The distribution of voids in the three concrete groups, Fig. 12, clearly shows that the area of small voids (0.2–1.6 mm) in mould-cast concrete was very much greater than that of both poor and good printing concrete. The poorly printed had more large voids (1.6–4.0 mm) compared with mould-cast concrete and are mostly located between printed filaments (Fig. 7). Once these were eliminated by correctly controlling the printing path and concrete rheology, the density increased as seen in the well printed concrete (2350 kg/m^3) that is representative of the specimens prepared for the other hardened property tests. The distribution of voids in good printing concrete agreed well with this as the area of 0.2–4.0 mm voids was significantly lower than both mould-cast and poor printing concrete.

Whilst the tests reported here are not extensive they provide important insights into the nature of this extrusion process and the influence on the structure of the resulting matrix and hence mechanical performance.

3.6. Drying shrinkage

As expected, the concrete cured in water shrank the least. It expanded up to 67 microstrain in first two days and then shrank to 177 microstrain by 28 days. Thereafter the shrinkage rate noticeably reduced with only 62 microstrain between 30 and 180 days (Fig. 13). The influence of damp hessian was monitored in two phases. During the first 60 days it was watered and wrapped in plastic sheeting so the relative humidity was around 100% but the temperature varied in a range of 15 to 25 °C depended on the ambient conditions. The shrinkage of 252 microstrain by 70 days was relatively low. In the second phase when the hessian was not watered and the plastic sheeting removed, the shrinkage rate increased from 70 to 90 days (408 microstrain), then gradually slowed to 570 microstrain at 184 days. The concrete in the climatic chamber at a consistent 20 °C and 60% relative humidity shrank quickly in first 30 days by 597 microstrain then gradually slowed to 855 microstrain at 189 days.

The higher shrinkage, by a factor of 3–4 times larger than that cured at 100% relative humidity, agrees reasonably well with the research by Bissonnette et al. [31] who observed the influence of relative humidity on the drying shrinkage of a mortar and obtained the results of approximately 300, 800 and 1400 μm for the specimens cured in 92, 75 and 48% relative humidity, respectively. Brooks et al. [32] also found greater shrinkage in 30 MPa compressive strength mortar specimens cured under plastic sheeting (approximately 2200 μm) compared with water (approximately 1000 μm). The results are thus as would be expected of cementitious system sensitive to changes in relative humidity, which disturb the equilibrium between adsorbed water and vapour pressure [33].

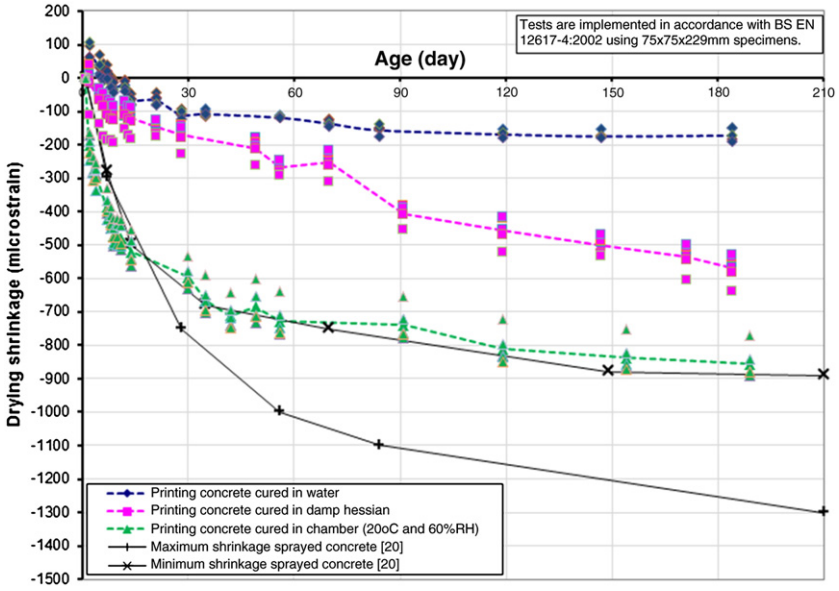

Fig. 13. Drying shrinkage in three curing conditions with comparison to sprayed concretes.

The shrinkage in all three conditions was notably lower than that of sprayed mortars [19,20] considered to be low shrinkage materials, when cured at 20 °C and 50% relative humidity. The optimum particle grading, low water/binder ratio and fly ash addition thus appeared to be helpful in lowering the shrinkage of the high performance printing concrete. This is a notable advantage for a manufacturing process without formwork where the complete surface of components is exposed.

4. Conclusions

A high-performance concrete has been successfully developed for a digitally-controlled printing process which can build architectural and structural components without formwork. The concrete in the mould-cast state had high strengths (107 and 11 MPa compressive and flexural strength respectively), low drying shrinkage and a density of 2250 kg/m^3. The printing process increased the density up to 2350 kg/m^3, although, as anticipated, the layering process can introduce small linear voids in the interstices between the extruded filaments. The gentle vibration of concrete container and the small pump pressure in the extrusion process probably reduced the volume of voids, resulting in the increase in density. Furthermore, poor printing could result in a lower density (2260 kg/m^3) with 1.6–4.0 mm voids located principally at the intersection of filaments.

The hardened properties were inevitably affected by any anisotropy in the layered structure of freeform components. Up to 30% reduction in compressive strength was observed in a curvy-shape full-scale bench structure. The potential improvement is implied by the higher strengths of around 91–102 MPa found in the specimens extracted from straight-line printed slabs. Here the reduction was only 5–15%, depending on the orientation of the loading relative to the layers, the lowest strengths occurring as would be expected when loading in planes parallel to the layers.

In terms of tensile properties, the flexural strength was significantly higher (13–16 MPa) than the mould-cast control (11 MPa) when tension was aligned with the extruded filaments. However, as expected, the flexural strength was significantly reduced when loaded to cause tension between (perpendicular) the layers (by up to 36%) but still high relative to conventional precast concretes at 7 MPa. A similar trend was observed in the measurement of direct tensile strength, reducing from 3.0 MPa in the mould-cast control to 2.3 MPa, the difference between the indirect and direct values following well-established behaviour.

The bond strength between the layers of printed concrete is perhaps the critical mechanical property of material produced by an AM process, creating potential flaws between extrusions that induce stress concentrations. This is highly dependent on the adhesion which is a function of the time between extrusions. There is a careful balance required, as with sprayed concretes, keeping the materials sufficiently open for adhesion, but developing sufficient rigidity to support its self-weight. The optimised mix contained appropriate proportions of superplasticizer and retarder.

The tensile bond strength inevitably reduced as the printing gap between layers increased. Where this was kept to 15 min the bond was greater than the tensile capacity of the material. A gap of 30 min or more resulted in bond failure at the interface and a relationship between characteristic bond strength and time has been established.

In macro terms, a variety of freeform building components were printed, including a large-scale curvy bench with weight of approximately 1 tonne [7,8]. Whilst drying shrinkage of such parts is inevitably a concern, the data indicates acceptable levels when good curing is provided. The research has thus demonstrated the potential of concrete printing as a viable new production process that can introduce greater geometric freedom into the design process as well as offering a novel means of manufacture that could avoid the need to mass produce identical concrete parts with limited numbers of variants. Further research is required to assess the structural behaviour of such components under simulated service conditions as well as to establish their durability, particularly in relation to any adverse effects of the layering process.

Acknowledgements

This project was funded by the Engineering and Physical Sciences Research Council under grant EP/E002323/1 through the IMCRC at Loughborough University. The authors acknowledge the supply of materials from Hanson Cement, Weber (St Gobain) and BASF and the assistance in designing the freeform components from Foster & Partners and Buro Happold. We are also grateful for the laboratory assistance of John Webster, Gregory Courtney, Harriet Mather, Jonathan Hales and David Spendlove.

References

[1] R.A. Buswell, R.C. Soar, A.G.F. Gibb, T. Thorpe, Freeform construction: mega-scale rapid manufacturing for construction, Autom. Constr. 16 (2007) 224–231.
[2] S. Lim, T. Le, J. Webster, R. Buswell, S. Austin, A.G.F. Gibb, T. Thorpe, Fabricating construction components using layer manufacturing technology, Proceedings of International Conference on Global Innovation in Construction, Loughborough, UK, 2009, pp. 512–520.
[3] H. Okamura, M. Ouchi, Self-compacting concrete, J. Adv. Concr. Technol. 1 (2003) 5–15.
[4] RILEM Technical Committee, Final report of RILEM TC 188-CSC "Casting of self compacting concrete", Mater. Struct. 39 (2006) 937–954.
[5] S.A. Austin, P. Robins, C.I. Goodier, The rheological performance of wet-process sprayed mortars, Mag. Concr. Res. 51 (1999) 341–352.
[6] S.A. Austin, P. Robins, C.I. Goodier, Construction and Repair with Wet-Process Sprayed Concrete and Mortar, Technical Report, 56, The Concrete Society, UK, 2002, p. 44.
[7] T. T. Le T, S. A. Austin, S. Lim, R. Buswell, A. G. F. Gibb, T. Thorpe, Mix design and fresh properties for high-performance printing concrete, Materials and Structures (accepted for publication).
[8] T.T. Le, S.A. Austin, S. Lim, R. Buswell, A.G.F. Gibb, T. Thorpe, High-performance printing concrete for freeform building components, Proceedings of International Fib Symposium on Concrete Engineering for Excellence and Efficiency, Prague, Czech Republic, 2011, pp. 499–502.
[9] B. Khoshnevis, D. Hwang, K. Yao, Z. Yeh, Mega-scale fabrication by contour crafting, Int. J. Ind. Syst. Eng. 1 (2006) 301–320.
[10] Dini Enrico, D_Shapeaccessed on, http://www.d-shape.com05th October 2011.
[11] A.M. Evans, R.I. Campbell, A comparative evaluation of industrial design models produced using rapid prototyping and workshop-based fabrication techniques, Rapid Prototyping J. 9 (2003) 344–351.
[12] C. Fernando, in: Elnashar Magdy (Ed.), Fabrication of HA/PLLA Composite Scaffolds for Bone Tissue Engineering Using Additive Manufacturing Technologies, Biopolymers, ISBN: 978-953-307-109-1, 2010, pp. 227–242.
[13] World Technology Evaluation Center, Inc., Additive/Subtractive manufacturing research and development in Europe, WTEC Panel report, 2004, p. 154.
[14] British Standards Institution, BS EN 12390–3:2009 Testing Hardened Concrete — Compressive Strength of Test Specimens, Milton Keynes, UK, 2009, p. 15.
[15] British Standards Institution, BS EN 12390–5:2009 Testing Hardened Concrete — Flexural Strength of Test Specimens, Milton Keynes, UK, 2009, p. 11.
[16] British Standards Institution, BS EN 14488–4:2005+A1:2008 Testing Sprayed Concrete — Bond Strength of Cores by Direct Tension, Milton Keynes, UK, 2008, p. 7.
[17] British Standards Institution, BS EN 12617–4:2002 products and systems for the protection and repair of concrete structures. Test methods, Determination of Shrinkage and Expansion, Milton Keynes, UK, 2002, p. 14.
[18] British Standards Institution, BS EN 12390–7:2009 Testing Hardened Concrete — Density of Hardened Concrete, Milton Keynes, UK, 2009, p. 10.
[19] S.A. Austin, P. Robins, C.I. Goodier, The performance of hardened wet-process sprayed mortars, Mag. Concr. Res. 52 (2000) 195–208.
[20] C.I. Goodier, S.A. Austin, P. Robins, Low-volume wet-process sprayed concrete: hardened properties, Mater. Struct. 41 (2008) 99–111.
[21] American Concrete Institute, ACI 212.4R-93 (Reapproved 1998) Guide for the Use of High-Range Water-Reducing Admixtures (Superplasticizers) in Concrete, 1998, p. 10.
[22] UK Cement Admixtures Association, Admixture Technical Sheet — ATS 2 Superplasticising/High Range Water Reducing, 2006, p. 5.
[23] British Standards Institution, BS EN 12504–1:2009 Testing Concrete in Structures Part 1: Cored Specimens — Taking, Examining and Testing in Compression, 2009, p. 8.
[24] J.R. Del Viso, J.R. Carmona J R, G. Ruiz, Shape and size effects on the compressive strength of high-strength concrete, Cem. Concr. Res. 38 (2008) 386–395.
[25] A.M. Neville, Properties of Concrete, Longman group limited, England, UK, 1995.

[26] T. T. Le, Ultra high performance fibre reinforced concrete paving flags, PhD thesis, University of Liverpool, UK, 2008, p. 405.
[27] S. Bhanjaa, B. Sengupta, Influence of silica fume on the tensile strength of concrete, Cem. Concr. Res. 35 (2005) 743–747.
[28] S.A. Austin, P. Robins, Y. Pan, Tensile bond testing of concrete repairs, Mater. Struct. 28 (1995) 249–259.
[29] Department of Transportation, United States, Tensile Bond Strength of a High Performance Concrete Bridge Deck Overlay — Field Test Report, Federal Highway Administration, Office of Pavement Technology, Washington, USA, 2000, p. 10.
[30] K.H. Hindo, In-plane bond testing and surface preparation of concrete, Concr. Int. 12 (4) (1990) 46–48.
[31] B. Bissonnette, P. Pierre, M. Pigeon, Influence of key parameters on drying shrinkage of cementitious materials, Cem. Concr. Res. 29 (1999) 1655–1662.
[32] J.J. Brooks, B.H. Abu Bakar, Shrinkage and creep of masonry mortar, Mater. Struct. 37 (2004) 177–183.
[33] K. Kovler, S. Zhutovsky, Overview and future trends of shrinkage research, Mater. Struct. 39 (2006) 827–847.